Evaluation of dynamical models: Dissipative synchronization and other techniques

Luis Antonio Aguirre,* Edgar Campos Furtado, and Leonardo A. B. Tôrres
Laboratório de Modelagem, Análise e Controle de Sistemas Não-Lineares, Programa de Pós-Graduação em Engenharia Elétrica, Universidade Federal de Minas Gerais, Avenue Antônio Carlos 6627, 31270-901 Belo Horizonte, Minas Gerais, Brazil
(Received 15 September 2005; revised manuscript received 28 August 2006; published 13 December 2006)

Some recent developments for the validation of nonlinear models built from data are reviewed. Besides giving an overall view of the field, a procedure is proposed and investigated based on the concept of dissipative synchronization between the data and the model, which is very useful in validating models that should reproduce dominant dynamical features, like bifurcations, of the original system. In order to assess the discriminating power of the procedure, four well-known benchmarks have been used: namely, Duffing-Ueda, Duffing-Holmes, and van der Pol oscillators, plus the Hénon map. The procedure, developed for discrete-time systems, is focused on the dynamical properties of the model, rather than on statistical issues. For all the systems investigated, it is shown that the discriminating power of the procedure is similar to that of bifurcation diagrams—which in turn is much greater than, say, that of correlation dimension—but at a much lower computational cost.

DOI: 10.1103/PhysRevE.74.066203 PACS number(s): 05.45.Tp, 05.45.Xt, 07.05.Tp, 07.05.Kf

I. INTRODUCTION

Model building from data has been of great interest for many years within the community of nonlinear dynamics since one of the first works in this field [1]. For the last 20 years or so, many different procedures have been put forward for building nonlinear models from data. In a sense, the field of model building is now rather mature within the community of nonlinear dynamics.

After building a model it is important to know if such a model is in fact a dynamical analog of the original system. An answer to that question is searched for during model validation. Among the several issues concerning model building, model validation is probably the one that has received the least attention. For instance, in [2] an interesting discussion of several aspects of global modeling is found; however, model validation is hardly mentioned.

Many of the tools for model validation that were commonly used by the mid-1990s were investigated and compared in [3]. The main conclusion of such a work was that if a global model of a system is required, then one of the most exacting procedures for model validation is to compare the model bifurcation diagram to that of the true system. Two similar diagrams[1] point to two entities (usually system and model) which display the same dynamical regimes over a rather wide range of parameter values. In fact it is widely acknowledged that bifurcation diagrams "are one of the most informative forms of presentation of dynamical evolution" [4]. On the other hand, quantities such as dimension measures, Lyapunov exponents, phase portraits, and so on can only quantify attractors and actually say very little about the model ability to mimic the system as it evolves from one dynamical regime (attractor) to another. Thus, good models should match closely such geometrical invariants; however, that matching is insufficient on its own to guarantee the quality of such models [5]. In fact, it is known that even two drastically different attractors may have similar fractal dimension or Lyapunov exponents.

Although bifurcation diagrams provide a very exacting means of verifying the dynamical overall behavior of a model, their practical use is somewhat limited to those cases in which it is viable to obtain such a diagram for the original system.[2] Another practical difficulty is that model validation using bifurcation diagrams is generally quite subjective, as will be illustrated in Sec. IV. In addition, the numerical determination of bifurcation diagrams could become rather demanding. In order to overcome such shortcomings of the bifurcation diagrams as a tool for model selection, this paper proposes a way of choosing from a set of candidate models based on dissipative synchronization. To assess the performance of the our method, bifurcation diagrams are used because they are known to be a hard test when the model dynamics are in view. Having said that, it is worth pointing out that bifurcation diagrams have been used in model validation in several contexts [6–16], where in some cases the systems were *autonomous* (i.e., had no, time-dependent, exogenous variables).

The remainder of the paper is organized as follows. Section II surveys some of the most commonly used methods of model validation applied to nonlinear dynamics. In that section three rather recent developments are mentioned in some detail. In Sec. III a procedure for model evaluation is presented. This procedure is based on dissipative synchronization. The ideas are tested using three benchmark systems, and the performance of the synchronization scheme is compared to that of other methods in Sec. IV. The main conclusions of the paper are provided in Sec. V.

*Corresponding author. FAX: +55 31 3499-4850. Email address: aguirre@cpdee.ufmg.br

[1] By *similar* it is meant that both model and system undergo the same sequence of bifurcations and display the same dynamical regimes for approximately the same values of the bifurcation parameter.

[2] A very interesting example has been published recently by Small and coworkers who have discussed the estimation of a bifurcation diagram from a set of biomedical data [77].

II. OVERVIEW OF SOME METHODS

In this section the aim is twofold. First, it is desired to provide a glance as to how several authors have proceeded in validating dynamical models. In browsing through the literature, only the last decade was of concern. The interested reader is referred to [3] for a coverage of the field up to the beginning of the 1990s. Second, three different approaches for model validation, which seem to be rather different in concept from the more "standard" procedures, will be briefly pointed out.

Before actually starting to describe some results in the literature, a few remarks are in order. First and foremost, the challenge of model validation or of choosing among candidate models should take into account the intended use of the model. Hence, a model could be good for one type of applications and, nonetheless, perform poorly in another. In the context of this paper, the main concern is to assess the model dynamics. A different concern, though equally valid, which would probably require a different approach, would be to assess the forecasting capabilities of a model. Second, it should be realized that two similar though different problems are (i) model validation, which usually aims at an *absolute* answer like valid or not valid and (ii) model selection, which usually aims at a *relative* answer such as model $\mathcal{M}_1$ is better than model $\mathcal{M}_2$ according to criterion $\mathcal{C}$. Finally, when it comes to model validation, the safest approach is to use many criteria, rather than just one.

Although very popular in other fields, the computation of various *measures of prediction errors* (one-step-ahead and free-run) in the case of nonlinear dynamical systems is not conclusive in what concerns the overall dynamics of the identified model [3,17,18], though it does convey much information on the forecasting capabilities of a model.

Subjective though it is, the *visual inspection of attractors* (or simply comparing the morphology of two time series) is still quite a common way of assessing the quality of models [18–32]. Such a procedure is not only subjective but also ineffective to discriminate between "close" models—that is, models with slight, but important, differences in their dynamical behavior. What renders this procedure subjective is the fact that no quantitative mechanism is used to compare how close are two reconstructed attractors. In this respect the work by Pecora and coworkers could be an alternative for determining how close the original and model attractors are [33]. To the best of our knowledge the statistic measures put forward in the mentioned paper have not yet been used in the context of model validation.

Still in relation to the visual inspection of attractors, it should be noticed that in many practical instances there is not much more that can be done consistently. For instance, in the case of slightly nonstationary data, to compare short-term predictions with the original data is basically the best that can be done. Building a model for which the free-run simulation approximates the original data in some sense is usually a nontrivial achievement.[3]

Other *attractor features* are still in common use when it comes to model validation. Among such features the following are frequently used:[4] Lyapunov exponents [17,34–38], correlation dimension [17,18,36], location and stability of fixed points [30,39,40],[5] Poincaré sections [17,41], geometry of attractors [42], attractor symmetry [6,43], first-return maps on a Poincaré section [44,45], probability density functions of recurrence in state space [46], and topological features such as linking numbers and unstable periodic orbits (UPO's) [47–49].

Before addressing a few rather recent techniques for model validation of nonlinear dynamics, it is important to mention that meaningful validation can only be accomplished by taking into account the intended use of the model. A model that provides predictions consistent with the observed data will probably not be a good model to study, say, the sequence of bifurcations of the original system. On the other hand, if a model is sought to forecast a given variable, the statistical properties of the forecasts are certainly more important than, for instance, to have the same linking numbers as the original attractor, assuming it exists.

A. Surrogate data hypothesis testing

A well-celebrated paper by Theiler and colleagues introduced to the community of nonlinear dynamics the application of surrogate analysis for hypothesis testing [50]. When that paper was published, the main concern was to distinguish low-dimensional chaos from noise. Surrogate-based techniques have since then multiplied in spite of many potential pitfalls [51]. However, as a whole, well-conceived surrogate analysis is an important tool to test for some specific features in the data.

Although estimations of the test statistics from model free-run simulations and the data had been generously used for model validation, Small and Judd were the first to suggest to compare such simulations in the framework of surrogate analysis [52]. The overall procedure put forward by these authors was to use estimated models to produce a large number of time series and to use some test statistic to try to assess if it is likely that the data could have been produced by a model (or models) such as those used to produce the surrogates. Although this procedure has not been duly exploited in the context of model validation, it seems to have great potential especially when the requirements on the models have a greater weight towards statistics rather than dynamics.

Of course, a key point in this procedure is the choice of the test statistic. For instance, suppose that the correlation dimension or the largest Lyapunov exponent is chosen to compare a set of free-run simulated data with the measured data. Suppose further that the null hypothesis is that the measured data are compatible with the estimated model. Even if

[3] In this respect we rather disagree with [56] who consider free-run simulation of models a trivial validity test.

[4] Some of such properties have been recently discussed in the context of model validation in [78].

[5] In particular, it has been shown that fixed-point stability of nonlinear models is consistent with breathing patterns found in real data [79].

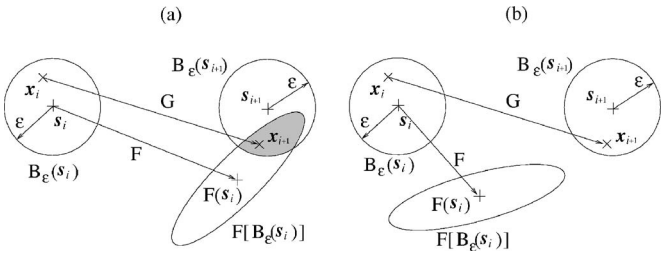

FIG. 1. Graphical interpretation of (a) consistent prediction and (b) inconsistent prediction [54]. In (a) the shaded region indicates that there is a subset of forecasts that are indistinguishable from the "true" state ($\boldsymbol{x}_{i+1}$) within observational uncertainty.

we cannot reject the null hypothesis, that does not guarantee equivalence of *dynamical* behavior because quite different attractors may have similar indices [53]. This is also true for the correlation dimension.

B. Embedding-space consistent predictions

Another recent contribution to model validation which, in a sense, is related to the one mentioned in the previous section has been described in [54] and has been named consistent nonlinear dynamics (CND) testing. In order to understand the main idea behind the procedure by McSharry and Smith, consider Fig. 1.[6]

Denote the "true" dynamics by $\mathbf{G}$ and a given model by $\mathbf{F}$. The "true" state at time i is indicated by $\boldsymbol{x}_i$; therefore, the true state at time $i+1$ can be expressed as $\boldsymbol{x}_{i+1}=\mathbf{G}(\boldsymbol{x}_i)$. It is also assumed that the observed state at time i is $\boldsymbol{s}_i$. The one-step-ahead prediction of model $\mathbf{F}$ starting from the last available observation is $\hat{\boldsymbol{s}}_{i+1}=\mathbf{F}(\boldsymbol{s}_i)$. The one-step-ahead prediction error, also termed residual, is therefore $\xi_i=\boldsymbol{s}_{i+1}-\mathbf{F}(\boldsymbol{s}_i)$. Further, it is considered that $\dim[\boldsymbol{x}_i]=\dim[\boldsymbol{s}_i]$ and that $\boldsymbol{s}_i$ is at the center of an observational uncertainty sphere of radius ϵ, denoted by $\mathbf{B}_\epsilon(\boldsymbol{s}_i)$. The uncertainty within $\mathbf{B}_\epsilon(\boldsymbol{s}_i)$ is assumed to be uniformly distributed and ϵ is assumed known.

Starting from the sphere $\mathbf{B}_\epsilon(\boldsymbol{s}_i)$, model $\mathbf{F}$ is used to iterate $\mathbf{B}_\epsilon(\boldsymbol{s}_i)$ one step ahead. In practice, a finite number of potential states within $\mathbf{B}_\epsilon(\boldsymbol{s}_i)$ are produced and model $\mathbf{F}$ is iterated once starting from each one of such states. Because of different rates of stretching in phase space, the sphere $\mathbf{B}_\epsilon(\boldsymbol{s}_i)$ is deformed into $\mathbf{F}[\mathbf{B}_\epsilon(\boldsymbol{s}_i)]$, which will only be an ellipsoid if the dynamics is locally linear, but there is no need for this assumption unless computation time is a problem and more efficient schemes are required [54]. In Fig. 1, $\mathbf{F}[\mathbf{B}_\epsilon(\boldsymbol{s}_i)]$ is drawn as an ellipse only for convenience.

The region in phase space denoted by $\mathbf{F}[\mathbf{B}_\epsilon(\boldsymbol{s}_i)]$ is the region where the true state at time $i+1$ is likely to be found given the model $\mathbf{F}$, the observed initial condition $\boldsymbol{s}_i$, and the uncertainty radius ϵ associated with that observation. Now, at time $i+1$ another observation of the state becomes available $\boldsymbol{s}_{i+1}$ and, *assuming that the uncertainty radius* ϵ *has not changed*, $\mathbf{B}_\epsilon(\boldsymbol{s}_{i+1})$ denotes the region in phase space where the "true" state $\boldsymbol{x}_{i+1}$ is likely to be found. Therefore, if there is any intersection of $\mathbf{F}[\mathbf{B}_\epsilon(\boldsymbol{s}_i)]$ with $\mathbf{B}_\epsilon(\boldsymbol{s}_{i+1})$, there is no reason to disqualify the prediction $\mathbf{F}(\boldsymbol{s}_i)$ given the observation uncertainty. In that case it is said that prediction $\mathbf{F}(\boldsymbol{s}_i)$ is consistent. This case is illustrated in Fig. 1(a), whereas the case of inconsistent predictions is shown in Fig. 1(b).

This procedure is similar to the ideas mentioned in Sec. II A. The propagation of a large number of potential states within $\mathbf{B}_\epsilon(\boldsymbol{s}_i)$ corresponds to producing surrogate forecasts $\mathbf{F}[\mathbf{B}_\epsilon(\boldsymbol{s}_i)]$, and checking if there is any intersection of $\mathbf{F}[\mathbf{B}_\epsilon(\boldsymbol{s}_i)]$ with $\mathbf{B}_\epsilon(\boldsymbol{s}_{i+1})$ amounts to verifying if the data are significantly different from the surrogates. The main differences seem to be basically two. First, the test statistic in the procedure proposed in [54] is the residual whereas in the case of surrogate analysis there are quite a few options. Second, the verification of the significance of the test statistic is carried out in a rather geometrical setting in the case of CND testing, rather than the more statistical procedure in the case of surrogate analysis. On the other hand, the discussed version of CDN testing seems less demanding from a numerical point of view[7] and the procedure does provide state-dependent information, a benefit not readily available with surrogate analysis.

Before moving on it is vital to realize that the observational uncertainty ϵ plays a critical role in this procedure. In order to end up with meaningful results, there must be a reliable way of estimating ϵ. Otherwise, virtually *any* model can be made to provide consistent predictions by unduly increasing ϵ.

C. Synchronization

As done in Sec. II B, let us denote the "true" dynamics by $\mathbf{G}$ and a given model by $\mathbf{F}$. However, in the present section it is assumed that the dynamics are continuous—that is [55],

$$\frac{d\boldsymbol{x}}{dt}=\mathbf{G}(\boldsymbol{x}),$$

$$\frac{d\boldsymbol{y}}{dt}=\mathbf{F}(\boldsymbol{y})-\mathbf{E}(\boldsymbol{y}-\boldsymbol{x}), \tag{1}$$

where it has been assumed that $\dim[\boldsymbol{x}]=\dim[\boldsymbol{y}]$ and where the matrix $\mathbf{E}$ denotes the coupling between the true system and the model. The scheme illustrated in (1) will be referred to as dissipative synchronization.

The rationale behind this procedure is as follows. Assume the data $\boldsymbol{x}$ lie on a chaotic attractor. In many situations, provided $\mathbf{E}$ is adequately chosen and $\mathbf{G}=\mathbf{F}$, $\boldsymbol{y}\rightarrow\boldsymbol{x}$. That is, the model will synchronize to the system. In this case all the conditional Lyapunov exponents associated with (1) become negative.

If $\mathbf{G}$ and $\mathbf{F}$ differ slightly, the error $\boldsymbol{e}=\boldsymbol{y}-\boldsymbol{x}$ will not go to zero but will stay around the origin of the error space. The average distance to the origin of such a space will depend on $\mathbf{G}(\boldsymbol{x})-\mathbf{F}(\boldsymbol{x})$. Therefore such a distance (which in practice is a

[6]Both Fig. 1 and the nomenclature are based on [54].

[7]More sophisticated alternatives are discussed in [54].

measure of quality of "synchronization") is a measure of how far the estimated model **F** is from the true dynamics **G** [55].

In order to implement this scheme in practice the authors suggested taking matrix **E** to be diagonal with only one element different from zero. The authors then compare $|\boldsymbol{x}-\boldsymbol{z}|$ — where $\boldsymbol{z}$ is the model state vector *without* any driving force to $|\boldsymbol{x}-\boldsymbol{y}|$. If $|\boldsymbol{x}-\boldsymbol{y}|$ drops below a certain threshold (10^{-2} was used in [56]) and is "clearly" smaller than $|\boldsymbol{x}-\boldsymbol{z}|$—that is, $\boldsymbol{x}\approx\boldsymbol{y}$—and it is assumed that the model is synchronized to the data, **F** should therefore be sufficiently close to **G**.

As often happens in the realm of model validation, this procedure also is highly subjective, since it requires an *ad hoc* threshold, mentioned in the previous paragraph. In what concerns dissipative synchronization, it is well known that in many cases by increasing the strength of the coupling (matrix **E**) it is possible to force a greater degree of synchronization and, in some cases, even attain identical synchronization [55]. For instance, in [56] the authors found that for values of the coupling greater than 2, models of an electronic circuit would synchronize with the measured data. On the other hand, Letellier *et al.* [57] have found a lower bound of 0.1 for the coupling strength in order to guarantee synchronization between the Rössler system and perturbed versions of the original equations. It therefore becomes clear that it is sometimes possible to synchronize even a poor model to the data as long as the coupling strength is made sufficiently large. In fact, is has been shown that even different systems can synchronize, at a rather high cost [58].

Therefore although the concept of synchronization could be useful in the context of model validation, it becomes apparent that some adjustments are required to render the procedure more practical. Some steps in this direction will be given in the next section. Before, it is noted that synchronization has been used in parameter estimation problems [16,59–61].

III. DATA-MODEL SYNCHRONIZATION FOR DISCRETE MODELS

In this section a procedure based on dissipative synchronization is proposed in the context of model evaluation. Compared to the first procedure put forward in [55], the present method is different at least in three important aspects. First, the method has been developed for discrete-time models. Second, the criterion for evaluating a model is not if the model synchronizes (for the reasons discussed above) but rather is the *cost of synchronization*. Consequently, the synchronization scheme used does not seem to be critical since we aim at a *relative* evaluation of models rather than an *absolute* one.[8] Clearly, if the aim were to optimize synchronization, other synchronization schemes would have to be considered. It will be argued that better models cost less to synchronize with the data, with respect to dissipative synchronization. Therefore an index that measures the cost of maintaining models synchronized will be used; see Sec. III B. Third, in order to compare the cost of synchronization in a meaningful way, it is necessary to guarantee that the quality of the synchronization is similar. The following procedure will use the concept of *class of synchronization* defined in [62]; see Sec. III C.

A. Main motivation

It is assumed that the available data are scalar and discrete sequences $x(k)$ (output) and $u(k)$ (input), for $k=1,2,\ldots,N$. In the case no input is measured, the procedure remains valid with $u(k)=0,\forall\ k$. It is assumed that the data are correctly described by

$$x(k)=g(\psi_{ux}(k-1)), \tag{2}$$

where $\psi_{ux}(k-1)$ is a vector composed of lagged values of the data x and u up to and possibly including instant $k-1$. It is not assumed that the embedding is regular, in the sense of [25]. Finally, g is an unknown function that relates all the variables in $\psi_{ux}(k-1)$ to the future output $x(k)$.

Analogously, it is assumed that a model[9] f has been obtained from the given data such that $x(k)=f(\hat{\psi}_{ux}(k-1))+\xi(k)$, where the deterministic one-step-ahead prediction of the model is $f(\hat{\psi}_{ux}(k-1))$ and $\xi(k)$ is an error function. In principle there is no need to assume that $\xi(k)$ is white or that is has a certain probability distribution. Here, $\hat{\psi}_{ux}(k-1)$ is the vector of model-independent variables. It is not assumed that $\psi_{ux}(k-1)$ and $\hat{\psi}_{ux}(k-1)$ include the same set of lags.

Initially, it is desired to verify if model f will synchronize with the observed data. To investigate this, the following dissipative synchronization scheme can be easily implemented:

$$x(k)=g(\psi_{ux}(k-1)),$$

$$\hat{y}(k)=f(\hat{\psi}_{ux}(k-1))-h(k-1), \tag{3}$$

where $h(k)=c(x(k)-\hat{y}(k))$ and $c\in\mathbb{R}$ is a constant. It is interesting to notice that in (3), besides the dissipative coupling term, direct substitution of $\hat{y}$ with x has taken place. In such a framework the one-step-ahead synchronization error (OSASE) is defined as

$$\begin{aligned} e(k)&=x(k)-\hat{y}(k)=g(\psi_{ux}(k-1))-[f(\hat{\psi}_{ux}(k-1))-h(k-1)]\\ &=c(x(k-1)-\hat{y}(k-1))+[g(\psi_{ux}(k-1))-f(\hat{\psi}_{ux}(k-1))]\\ &=ce(k-1)+\xi(k-1). \end{aligned} \tag{4}$$

It is instructive to see that Eq. (4) is fundamentally an ARX (autoregressive with an exogenous input) model. Therefore, the OSASE is a first-order autoregressive process driven by the "exogenous" variable $\xi(k-1)$. It is well known that in order to have a nondiverging process, $|c|<1$. More-

[8] This remark becomes even more important if we consider that in some cases it is possible to synchronize totally different systems [80].

[9] No assumptions are made concerning the type of model f apart from the fact that it should be a discrete-time model.

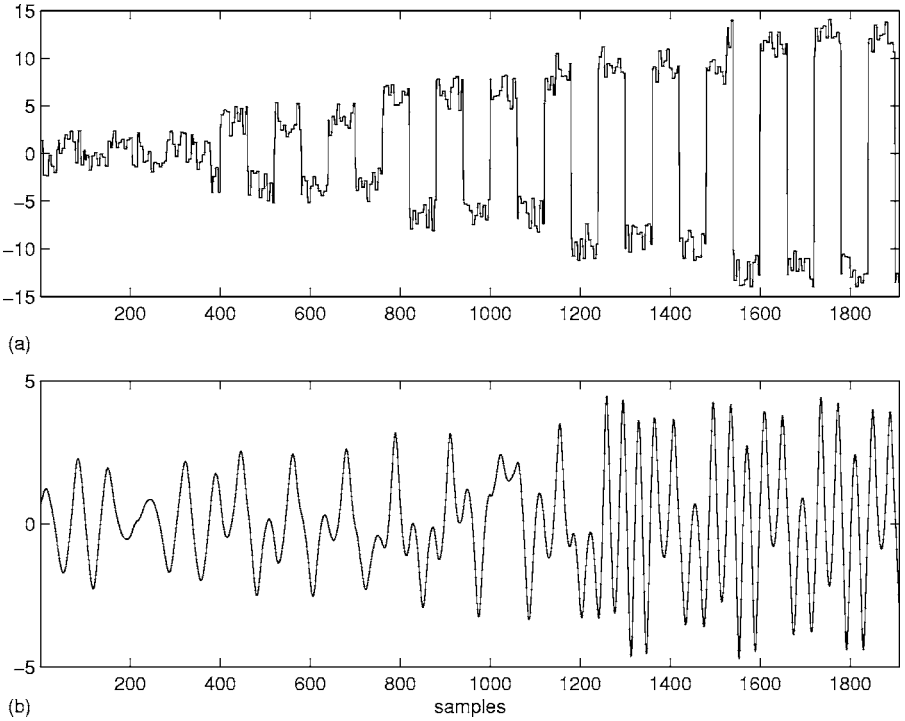

FIG. 2. Identification data for the Duffing-Ueda oscillator (a) input and (b) output. These data are used only for building models.

over, whereas the autonomous dynamics is governed by the dissipative coupling (the autoregressive part), the overall behavior is determined by the driving function $\xi(k-1)$ which is simply a measure of the distance between the dynamics underlying the data $g(\psi_{ux}(k-1))$ and the model $f(\hat{\psi}_{ux}(k-1))$. Clearly, should the difference between these entities be negligible, $\xi(k-1)\approx 0$ and $e(k)$ would naturally tend to zero, since $|c|<1$. Therefore, it is seen that the dynamical mismatch between $g(\psi_{ux}(k-1))$ and $f(\hat{\psi}_{ux}(k-1))$ is somehow reflected in the OSASE $e(k)$. Therefore $e(k)$ conveys important dynamical information and, at least in principle, it could be used as a measure of model quality. In this particular respect, the present procedure follows the main motivation in [55].

B. Cost of synchronization

In many systems synchronization is always possible as long as the coupling is sufficiently strong [55]. Because of this, it seems useless to declare valid a model that is forced to synchronize with the data. On the other hand, it is a fact that the closer two dynamical systems are, the easier it is to synchronize them. This last remark is taken to be our great motivation to define a measure of the cost of synchronization that later will be used to evaluate dynamical models.

The following working definition of cost of synchronization will be used:

$$J_{\mathrm{rms}}(c) = \lim_{N\to\infty} \sqrt{\frac{1}{N}\sum_{k=1}^{N} \|h(k)\|^2}, \tag{5}$$

where it is assumed that $k=1$ indicates the instant from which synchronization is achieved and not the first value in the data sequence. Viewing $h(k)=c(x(k)-\hat{y}(k))$ as the control action required to maintain the model synchronized to the data, it is possible to interpret $J_{\mathrm{rms}}(c)$ as the energy required to keep the model close to the data. It is stressed that in the practical computation of Eq. (5) the transients experienced by the model until it synchronizes with the data (if it ever does) are not taken into account. This is welcome in practice in so far as the effect of initial conditions is greatly diminished.

It should be noticed that there are many other ways in which the coupling (and therefore the cost of synchronization) can be defined. In particular [63] uses sinusoidal coupling and [64] uses sigmoidal coupling. The choice of $h(k)$ in this paper was made to keep the coupling as simple as possible. In fact, the choice of $h(k)$ is a linear approximation of the two nonlinear coupling schemes used in [63,64]. It is of paramount importance to remember that the aim in this work is *not* to achieve high-quality synchronization but rather to apply the *same* synchronization scheme to several systems and decide which synchronizes with similar quality at a lower cost. The following section will shed some light onto how to assess and quantify synchronization quality.

C. Class of synchronization

In order to compare cost of synchronization in a meaningful way, it will be necessary to guarantee that the quality of the synchronization is of a certain type. To this end, the concept of class of synchronization defined in [62] is adapted.

Two synchronized systems will belong to the ϵ class of synchronization if and only if

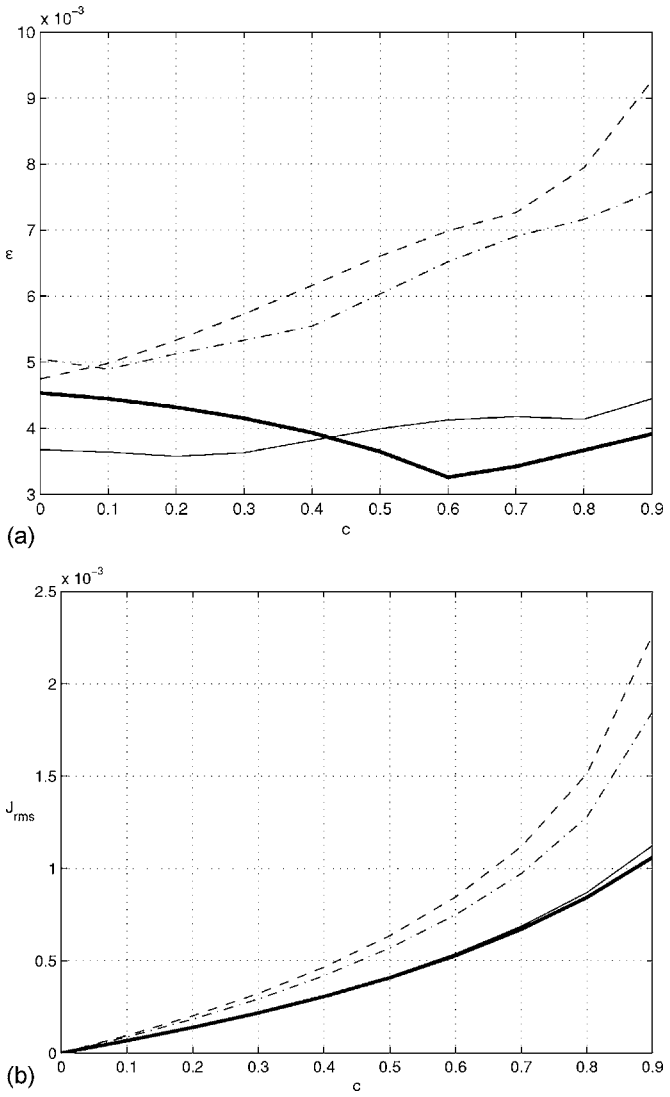

FIG. 3. (a) Maximum normalized synchronization error, $\epsilon_m(c)$ and (b) cost of synchronization for Duffing-Ueda models: (dot-dashed line) $\mathcal{M}_1$, (dashed line) $\mathcal{M}_2$, (solid line) $\mathcal{M}_3$, and (solid line, boldface) $\mathcal{M}_4$.

$$\frac{\sup\|e(k)\|}{\sup\|e(k)\|+1} < \epsilon(c), \quad \forall\ k \geq 1, \tag{6}$$

where $e(k)$ was defined in Eq. (4) and the dependence of the synchronization on the linear feedback gain c has been made explicit. It is clear that $0 \leq \epsilon(c) \leq 1$ and that $\epsilon(c) \approx 0$ implies $x(k) = \hat{y}(k)$ for that particular value of c. On the other hand, $\epsilon(c) \approx 1$ points to asynchronous behavior. For practical reasons, given a particular experiment for which a sequence of synchronization errors $e(k)$ is available, it is useful to consider the maximum normalized synchronization error, defined as

$$\frac{\max\|e(k)\|}{\max\|e(k)\|+1} = \epsilon_m(c), \quad \forall\ k \geq 1. \tag{7}$$

TABLE I. Largest Lyapunov exponent (λ) and correlation dimension (D_c) for the attractors obtained with $u(t) = 11\cos(t)$ and the models for the Duffing-Ueda system. The last column shows the average probability that the one-step-ahead predictions is within a dynamically consistent region and, within parentheses, the minimum and maximum values are given.

Model	λ	D_c	$\mathbf{B}_\epsilon(\boldsymbol{s}_{i+1}) \cap \mathbf{F}(\boldsymbol{s}_i)$
Original	0.11	2.29±0.019	
$\mathcal{M}_1$	0.09	2.31±0.001	99.8%(92–100)
$\mathcal{M}_2$	0.09	$2.24\pm4\times10^{-4}$	99.3%(63–100)
$\mathcal{M}_3$	0.10	2.31±0.002	100%(99–100)
$\mathcal{M}_4$	0.10	2.28±0.002	87%(29–100)

D. Comparing models

The procedure now being presented, as for most validation procedures, also has a certain degree of subjectivity. In view of this, rather than artificially trying to declare a certain model valid or not, the problem to be dealt with is to choose what seems to be the best model within a set of candidates. This has been referred to rather informally as *model evaluation* rather than *model validation*. The latter seems to suggest an "absolute" quality to the model, and it is arguable if that would be the best way of addressing the whole matter.

In comparing models, the two concepts presented in Secs. III B and III C, are important. Given two models that synchronize with the data in a similar way[10] the model with the "best dynamics" will typically be the one for which synchronization can be maintained at a lower cost. Because only one synchronization scheme (dissipative) is implemented, it could turn out that assessing models with another scheme would rank such a model in a different order. Though this could turn out to be true, it seems that it is not likely. Femat and coworkers, in a different setting, have varied the intensity (gain) of synchronization as well as model mismatch while computing a given performance index. For every synchronization case considered, models with less mismatch could always be recognized without ambiguity (there are no crossings in the performance plots; see their Fig. 4) [65].

The suggested approach to the problem is as follows. Suppose it is desired to choose among two models $\mathcal{M}_1$ and $\mathcal{M}_2$ the one with dynamics "closer to the dynamics underlying the data." First of all, the smallest maximum normalized synchronization error for each model is determined; that is, we search for $\epsilon_m^1(c_1) = \min[\epsilon_m^1(c)]$ and $\epsilon_m^2(c_2) = \min[\epsilon_m^2(c)]$, where the minimization is carried out over the range $0 < c < 1$. If the found values are quite different, the models can be ranked without further computations. However, if $\epsilon_m^1(c_1) \approx \epsilon_m^2(c_2)$, then the criterion to rank the models becomes the

[10] In this case we shall speak of two models that belong to the same class of synchronization or that have comparable maximum normalized synchronization errors.

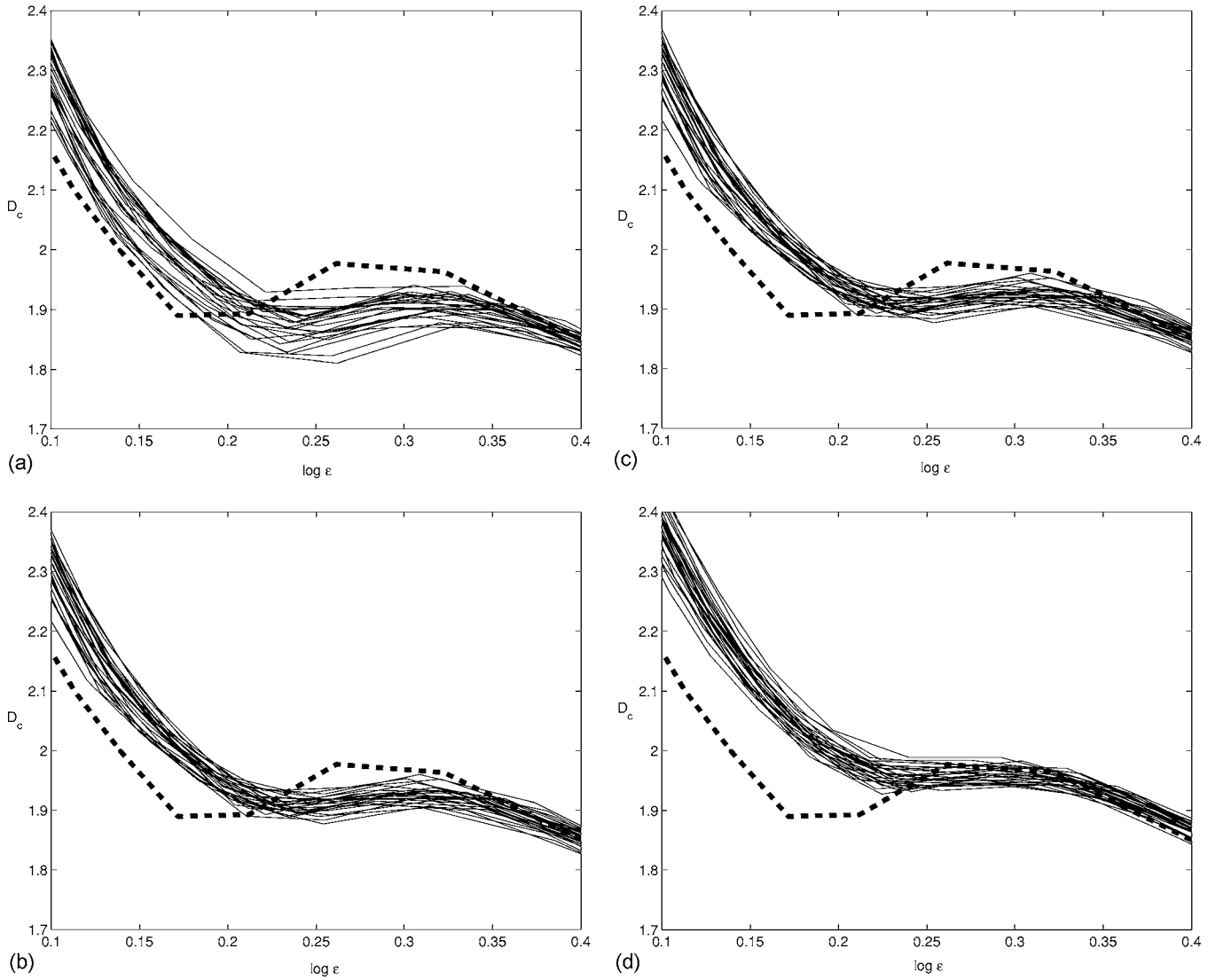

FIG. 4. Correlation dimension curves for the models. The x axis is, as usual, $\log_{10}\epsilon$. Each plot shows the curves for different realizations of the attractor at $A=11$, obtained initializing the models at different initial conditions. The thick dashed line is the curve that corresponds to the data produced by the differential equation (8): (a) $\mathcal{M}_1$, (b) $\mathcal{M}_2$, (c) $\mathcal{M}_3$, and (d) $\mathcal{M}_4$.

cost required to maintain models $\mathcal{M}_1$ and $\mathcal{M}_2$ at $\epsilon_m^1(c_1) \approx \epsilon_m^2(c_2)$—that is, $J_{\text{rms}}^1(c_1)$ and $J_{\text{rms}}^2(c_2)$, respectively. The model that achieves the smallest maximum normalized synchronization error at the lowest cost is likely to have better overall dynamics, as illustrated in the next section.

IV. NUMERICAL RESULTS

This section presents numerical examples that use well-known nonlinear oscillators.[11] As pointed out by Gilmore and Lefranc, the Duffing and van der Pol oscillators are among the basic testbeds used in the study of dynamical systems theory [66]. Also, the well-known Hénon map [67] will be used. In order to assess the effectiveness of the procedure put forward in Sec. III various aspects of the original systems and of the models will be compared.

A. Duffing oscillator

In the present section, two different versions of the Duffing oscillator will be investigated: the Duffing-Ueda oscillator [68] and the Duffing-Holmes oscillator [69]. The motivation for investigating both versions is simply that both versions of the Duffing oscillator have received attention in the literature. In addition to that, over the parameter range investigated in this paper, both versions present quite different behaviors.

1. Ueda equation

The Ueda version of the Duffing oscillator is [68]

$$\ddot{y} + k\dot{y} + y^3 = u(t). \tag{8}$$

[11]The data and code used are available from the authors on request.

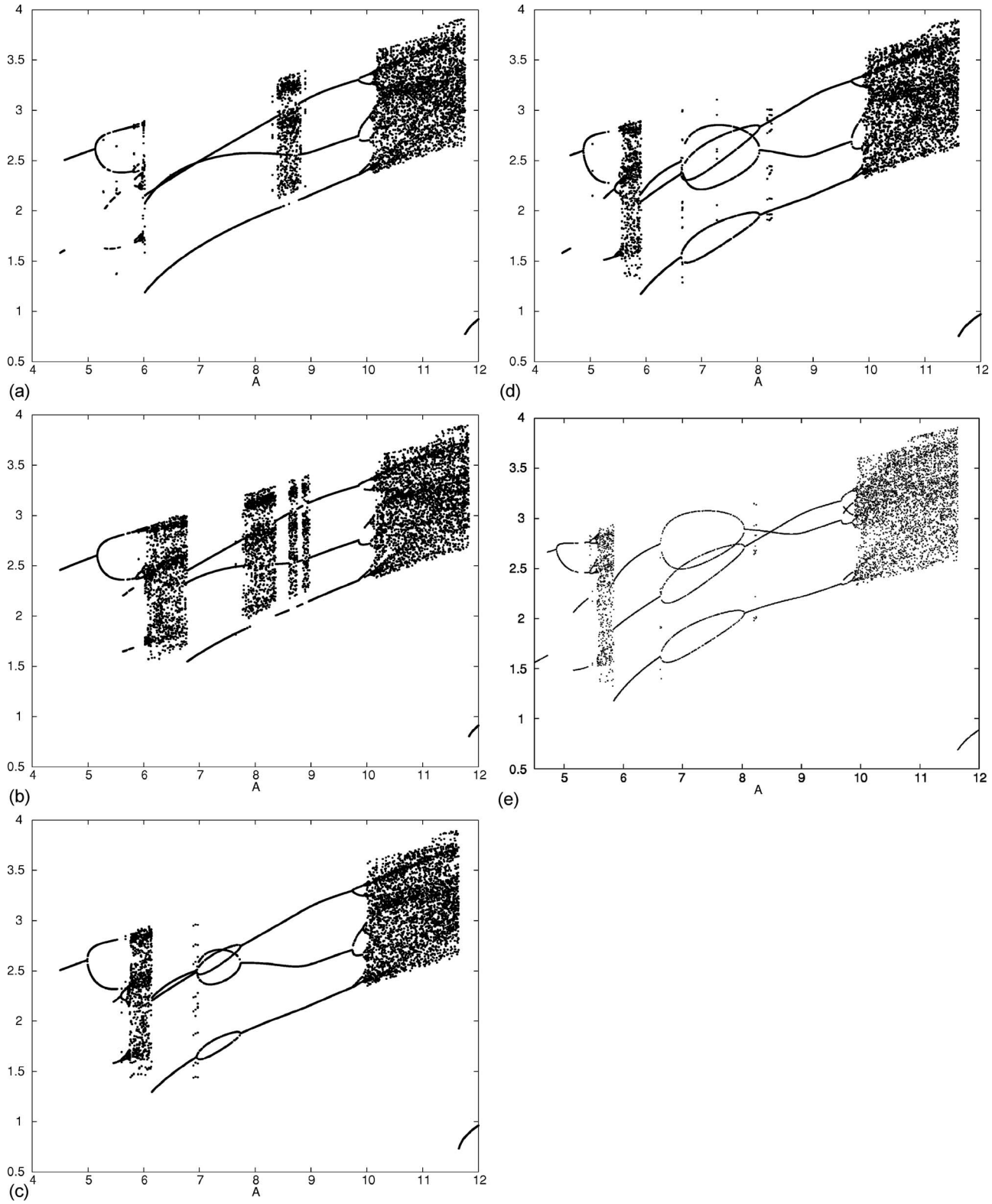

FIG. 5. Bifurcation diagrams with $u(t)=A\cos(t)$ and $4.5 \leq A \leq 12$ for (a) $\mathcal{M}_1$, (b) $\mathcal{M}_2$, (c) $\mathcal{M}_3$, (d) $\mathcal{M}_4$, and (e) original equation (8). $\mathcal{M}_4$ seems to be the best model in what concerns the sequence of bifurcations.

In this example, $k=0.1$. Equation (8) was simulated with the input $u(t)$ shown in Fig. 2(a), thus yielding the output shown in Fig. 2(b). Numerical in-tegration was carried out using a fourth-order Runge-Kutta algorithm with integration interval of $\pi/3000$. Subsequently the data were sampled at $T_s=\pi/60$ and used to obtain four models: $\mathcal{M}_1$, $\mathcal{M}_2$, $\mathcal{M}_3$, and $\mathcal{M}_4$.

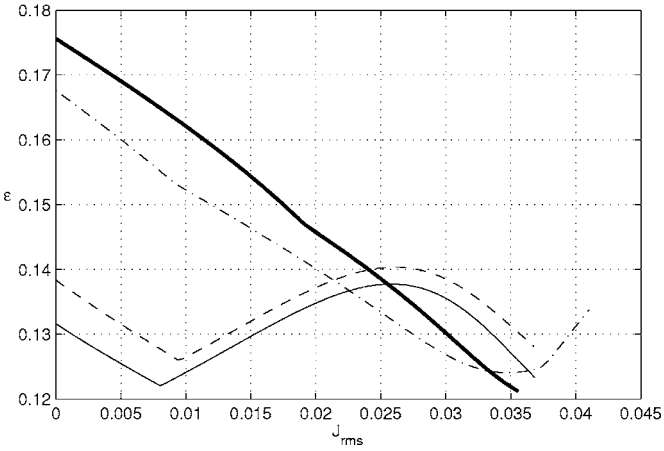

FIG. 6. Maximum normalized synchronization error $\epsilon_m(c)$ against the cost of synchronization, $J_{rms}(c)$, for Duffing-Holmes models: (dot-dashed line) $\mathcal{M}_1$, (dashed line) $\mathcal{M}_2$, (solid line) $\mathcal{M}_3$, and (solid line, boldface) $\mathcal{M}_4$. Each point on the lines corresponds to a particular value of c.

Figure 3 presents some results concerning the synchronization scheme discussed in Sec. III. First, Fig. 3(a) shows how the class of synchronization varies with the linear feedback parameter c. Second, Fig. 3(b) shows $J_{rms}(c)$—see Eq. (5) — for each value of c, which defines a class of synchronization.

From Fig. 3(a) it can be seen that the smallest maximum normalized synchronization error of model $\mathcal{M}_3$ is $\epsilon_m^3(c_3)\approx 3.6\times 10^{-3}$ ($c_3\approx 0.2$), whereas for $\mathcal{M}_4$ $\epsilon_m^4(c_4)\approx 3.2\times 10^{-3}$ ($c_4\approx 0.6$). As for the cost of synchronization, it is interesting to notice that although $J_{rms}^3(c)\approx J_{rms}^4(c)$ for the whole range of values of c, $J_{rms}^3(c_3)<J_{rms}^4(c_4)$. This poses a composite scenario (very common in multiobjective optimization) in which no Pareto solution is best in all the objectives. In this case, $\mathcal{M}_4$ is better in the sense that it attains the smallest synchronization class among all the models investigated. This means that it was able to attain the highest degree of synchronization. On the other hand, it can be seen that, considered at $c\approx 0.5$, model $\mathcal{M}_4$ attains the same value of the maximum normalized synchronization error as for model $\mathcal{M}_3$ at $c\approx 0.2$—that is, $\epsilon_m^3(0.2)\approx\epsilon_m^4(0.5)\approx 3.6\times 10^{-3}$. The analysis proceeds by verifying which of the two models achieves such a level of synchronization at a lower cost. In that respect it can be verified that $J_{rms}^3(0.2)<J_{rms}^4(0.5)$. In other words, $\mathcal{M}_3$ reaches a particular level of synchronization at a lower cost than $\mathcal{M}_4$. As a practical rule of thumb, the "clear" lowest maximum normalized synchronization error is used to rank models. More sophisticated criteria would be worth trying.

Table I shows the largest Lyapunov exponent and the correlation dimension computed for attractors of the original system and for the models. The last column in Table I shows the average probability that the one-step-ahead prediction is within a region consistent with the data. Minimum and maximum values are provided in parentheses. That is, $\mathbf{B}_\epsilon(\boldsymbol{s}_{i+1})\cap\mathbf{F}(\boldsymbol{s}_i)$ is a measure of the shaded region indicated in Fig. 1(a). To compute this value, *validation* data, with length $N=250$, were used. For each of those data points, 300 points—taken from a uniform distribution—within a hypersphere centered at $\boldsymbol{s}_i$ and with radius $\boldsymbol{\epsilon}$ were propagated using the model $\mathbf{F}$. Therefore, for each model 75 000 predictions were performed. Also, $\boldsymbol{\epsilon}$ was determined as twice the standard deviation of the uncertainty in the data.[12]

TABLE II. Largest Lyapunov exponent (λ) and correlation dimension (D_c) for the attractors obtained with $u(t)=0.3\cos(t)$ and the models for the Duffing-Holmes system.

Model	λ	D_c
Original	0.20	2.40±0.021
$\mathcal{M}_1$	0.18	2.35±0.002
$\mathcal{M}_2$	0.17	2.31±0.002
$\mathcal{M}_3$	0.19	2.38±0.001
$\mathcal{M}_4$	0.18	2.36±0.001

In this and future examples, the largest Lyapunov exponent was computed following [70] (for the case of known equations) and the correlation dimension was estimated using the algorithm discussed in [71].

Based on the results in Table I, it would be hard to choose a model. The clearest indication seems to be that model $\mathcal{M}_2$ is slightly inferior to the others, especially based on D_c, and that $\mathcal{M}_4$ is somewhat less consistent in what concerns one-step-ahead predictions.

Figure 4 shows the correlation dimension curves for 25 realizations obtained for each model (thin lines) and for the original data (thick dashed line) computed using the method described in [72]. All the time series were composed of 11 000 observations. To produce that figure the four models plus the original equation (8) were simulated for a sinusoidal input of frequency $\omega=1$ rad/s and $A=11$. The different realizations for the models were obtained by simulating the models from randomly chosen initial conditions taken on the attractor. From Fig. 4 it seems that models $\mathcal{M}_1$ and $\mathcal{M}_2$ are marginally acceptable if the first portion of the plots is considered. On the other hand, $\mathcal{M}_4$ would be the best model if the mid to last portions of the plots were considered. The subjectivity in choosing the working range in this procedure has already been pointed out [72].

Figure 5 shows the bifurcation diagrams for each model and the original system, obtained with $u(t)=A\cos(t)$. The procedure to produce such plots is quite intensive. On the other hand, it must be appreciated that a bifurcation diagram is of a much wider character than indices such as the largest Lyapunov exponent or the correlation dimension, which quantify one single attractor. Based on the bifurcation diagrams it seems fair to conclude that model $\mathcal{M}_4$ has the closest *overall* dynamics to the system. Unfortunately, it is very hard to reach this conclusion based on the data in Table I which cost far less to be estimated than the bifurcation dia-

[12]No noise was added to the data in this example. The uncertainty was quantified based on model residuals that are a by-product of the training stage. In this example such uncertainty was around 0.03% of the data.

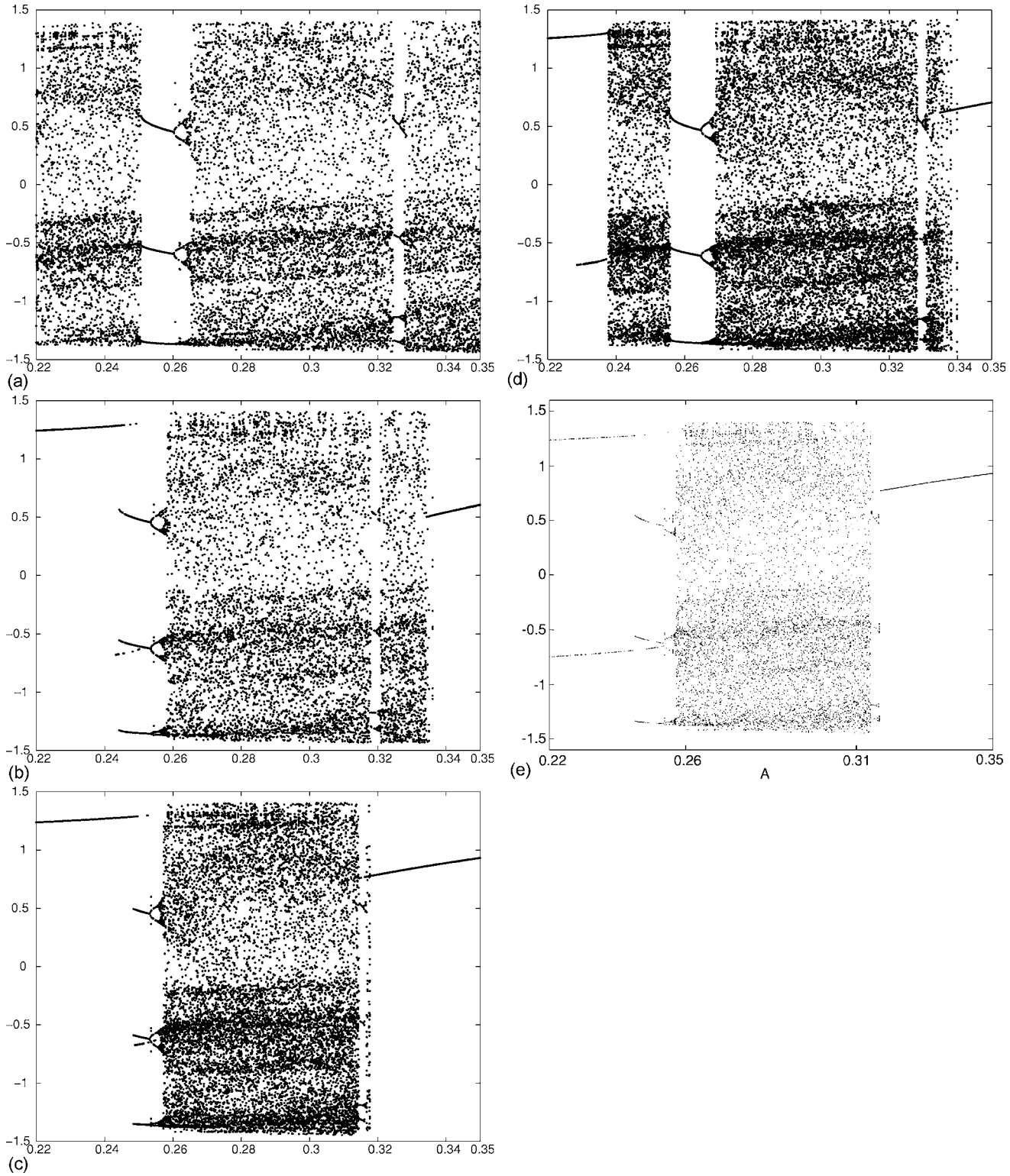

FIG. 7. Bifurcation diagrams with $u(t)=A\cos(t)$ and $0.22 \leq A \leq 0.35$ for (a) $\mathcal{M}_1$, (b) $\mathcal{M}_2$, (c) $\mathcal{M}_3$, (d) $\mathcal{M}_4$, and (e) original equation (9). Based on this figure, $\mathcal{M}_3$ seems to be the best model.

grams. Moreover, it is not always feasible to produce such diagrams for real systems.

Therefore, based on the proposed synchronization scheme and many other criteria, it seems adequate to state that models $\mathcal{M}_3$ and $\mathcal{M}_4$ are clearly superior to $\mathcal{M}_1$ and $\mathcal{M}_2$ in overall terms, and although $\mathcal{M}_3$ is quite competitive, $\mathcal{M}_4$ seems best overall.

As pointed out in Sec. III A, the model class of f is not taken into account in any part of the analysis. In the present and following examples the models used

TABLE III. Largest Lyapunov exponent (λ) and correlation dimension (D_c) for the attractors obtained with $u(t)=17\cos(4t)$ and the models for the van der Pol oscillator.

Model	λ	D_c
Original	0.33	2.44±0.001
$\mathcal{M}_1$	0.32	2.46±0.003
$\mathcal{M}_2$	0.34	2.53±0.001
$\mathcal{M}_3$	0.31	2.41±0.012

were nonlinear discrete-time polynomials. As a part of this first example, however, two additional neural-network multilayer perceptron models were considered.[13] One model was known to reproduce fairly well the original dynamics of the Duffing-Ueda oscillator whereas the other one not [6]. Following the procedure described in this paper the best network model did achieve a much lower maximum normalized synchronization error at a much smaller cost than the network with poor dynamical performance, thus confirming the scenario observed for models $\mathcal{M}_1$, $\mathcal{M}_2$, $\mathcal{M}_3$, and $\mathcal{M}_4$. Finally, it is mentioned that in [49] a continuous-time nonlinear polynomial model was obtained and made to synchronize by dissipative coupling. The authors validated such a model by means of topological analysis and suggested that the model topological validity was consistent with the fact that it was possible to synchronize it to the data. The fact that three different model classes showed consistency between synchronization and validation results suggests that the proposed procedure is, in fact, somewhat robust to the model class.

Before moving on, it is pointed out that in view of the results discussed in this example, in the next examples the CND testing and the correlation curves will be omitted and only nonlinear polynomial models will be considered.

2. Holmes equation

The Duffing-Holmes system is [69]

$$\ddot{y} + \delta\dot{y} - \beta y + y^3 = A\cos(\omega t). \tag{9}$$

As before, data were obtained by numerically integrating Eq. (9) with $\delta=0.15$, $\beta=1$, $A=0.3$, and $\omega=1$ rad/s, for which the system settles to a chaotic attractor. Data sampled at $T_s=\pi/15$ were used to obtain four models: $\mathcal{M}_1$, $\mathcal{M}_2$, $\mathcal{M}_3$, and $\mathcal{M}_4$.

The synchronization procedure discussed in Sec. III yielded the results summarized in Fig. 6. That figure shows the maximum normalized synchronization error (i.e., the estimated class of synchronization) against the cost of synchronization. Each point on the lines in that figure corresponds to a particular value of c. From Fig. 6 it is seen that although $\min[\epsilon_m^4(c)]$ is slightly smaller than $\min[\epsilon_m^3(c)]$, the cost of synchronizing $\mathcal{M}_3$ is significantly smaller than that of synchronizing $\mathcal{M}_4$. Therefore, Fig. 6 suggests that $\mathcal{M}_3$ is superior to $\mathcal{M}_4$, because it was possible to find a value of coupling such that the cost to synchronize $\mathcal{M}_3$ to the data with a certain quality is smaller than for $\mathcal{M}_4$ (and the other models). Another feature illustrated in that figure, is that $\mathcal{M}_2$ is similar to $\mathcal{M}_3$ in what concerns synchronization and the cost to maintain it.

[13]We thank Dr. Gleison Amaral for providing such models. See [6] for the details.

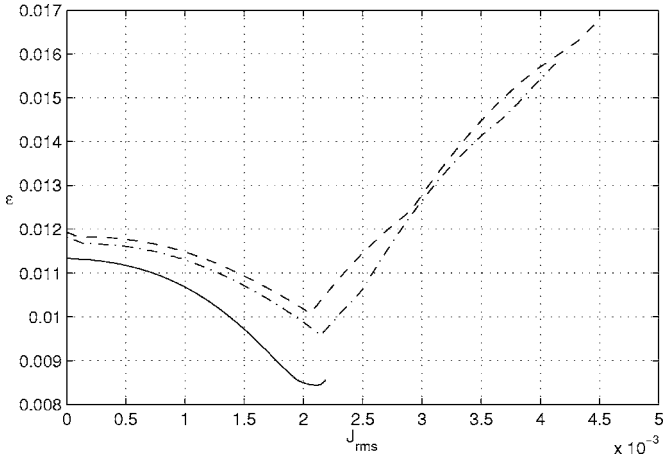

FIG. 8. Maximum normalized synchronization error $\epsilon_m(c)$ against the cost of synchronization, $J_{rms}(c)$, for van der Pol models: (dot-dashed line) $\mathcal{M}_1$, (dashed line) $\mathcal{M}_2$, and (solid line) $\mathcal{M}_3$. Each point on the lines corresponds to a particular value of c which was varied in the range $0\le c\le 0.9$.

The largest Lyapunov exponent and the correlation dimension of the models are shown in Table II. In view of the results for the Duffing-Ueda oscillator CND testing was not performed in the present example or in the next. From the data in the table, it seems that model $\mathcal{M}_2$ is slightly worse than the others. It is apparent that results such as those illustrated in Table II lack discrimination power.

The bifurcation diagrams shown in Fig. 7 suggest that $\mathcal{M}_2$ and $\mathcal{M}_3$ are the best, with $\mathcal{M}_3$ being somewhat superior. $\mathcal{M}_1$ and $\mathcal{M}_4$ have many spurious chaotic windows. All the models have a narrow periodic window which appears in the original system just before $A<0.32$. In the case of $\mathcal{M}_1$ and $\mathcal{M}_4$ such a window appears just after $A>0.32$. Models $\mathcal{M}_2$ and $\mathcal{M}_3$ present such a window just before $A<0.32$, as for the original system. $\mathcal{M}_2$, however, still presents a spurious chaotic window for $A>0.32$.

It is remarkable that, unlike for the Duffing-Ueda system, in the case of the Duffing-Holmes system (and also for the van der Pol oscillator as will be seen later) the input was a single-frequency signal and therefore the output, based on which the models were obtained, was on a single attractor. Nevertheless, such data do convey a great deal of information concerning how the original system bifurcates. In other words, although the model-building data were located at a single value of A in the bifurcation diagram, a rather wide range of values was successfully covered by the models.

B. van der Pol oscillator

This example considers the modified van der Pol oscillator [73]

$$\ddot{y} + \mu(y^2 - 1)\dot{y} + y^3 = u(t). \tag{10}$$

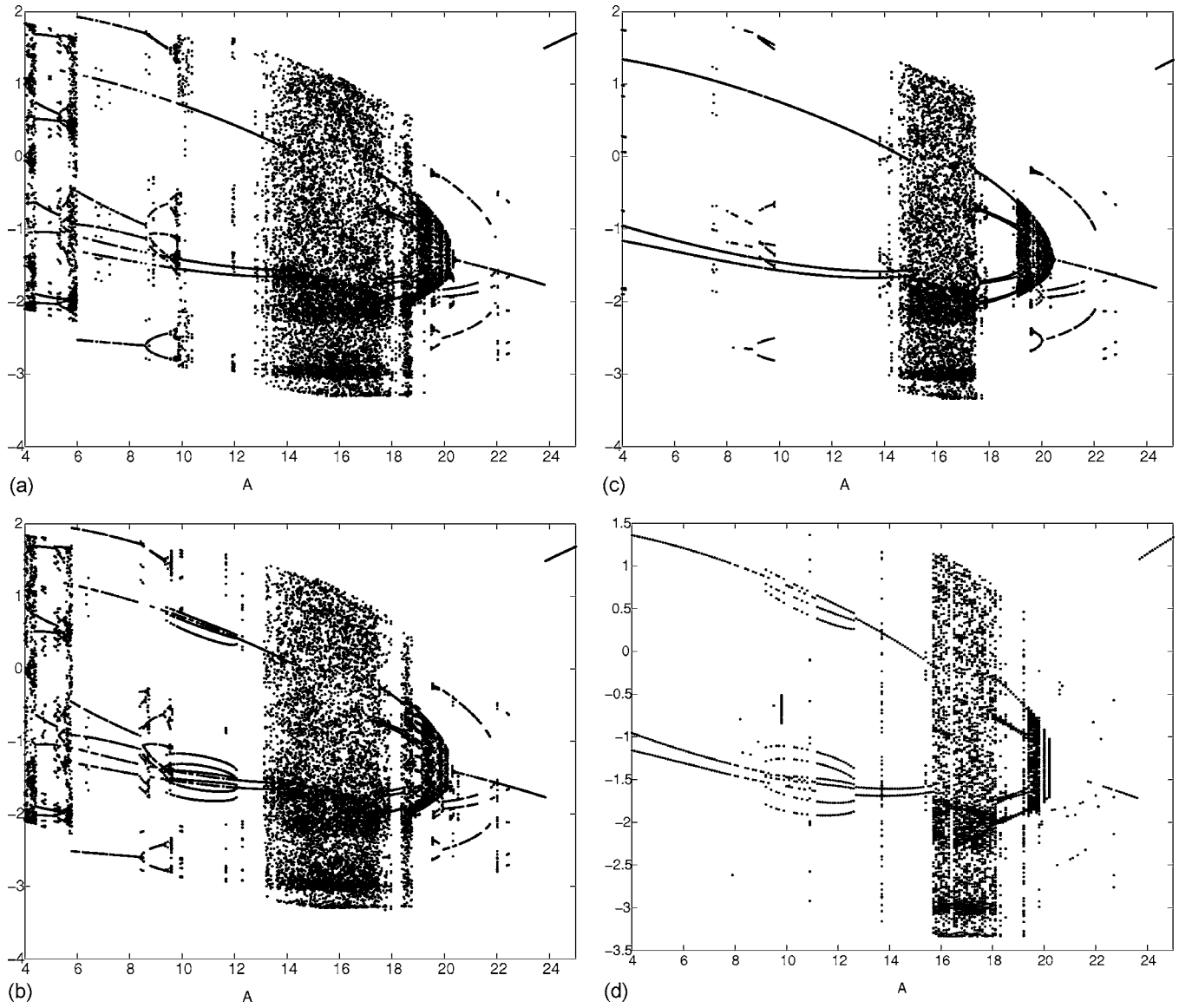

FIG. 9. Bifurcation diagrams with $u(t)=A\cos(4t)$ and $4\leq A\leq 25$ for (a) $\mathcal{M}_1$, (b) $\mathcal{M}_2$, (c) $\mathcal{M}_3$, (d), and original equation (10). $\mathcal{M}_1$ and $\mathcal{M}_2$ display several coexisting attractors. Based on this figure, $\mathcal{M}_3$ seems to have the diagram which is closest to that of the original oscillator.

Equation (10) was integrated with $\mu=0.2$, $u(t)=A\cos(\omega t)$, $A=17$, and $\omega=4$ rad/s, which yields a chaotic attractor. Data sampled at $T_s=\pi/80$ were used to obtain three models, $\mathcal{M}_1$, $\mathcal{M}_2$, and $\mathcal{M}_3$, for which the information on synchronization class and cost is summarized in Fig. 8. Such results suggest that $\mathcal{M}_3$ is probably the best overall model because, although the cost of synchronization is roughly the same for the three models (it is slightly smaller for $\mathcal{M}_3$), the maximum normalized synchronization error is significantly smaller for $\mathcal{M}_3$.

The largest Lyapunov exponent and the correlation dimension of models $\mathcal{M}_1$, $\mathcal{M}_2$, and $\mathcal{M}_3$ are shown in Table III. From the data in the table, it seems that model $\mathcal{M}_1$ is closest to the original system, with $\mathcal{M}_3$ being also quite good and $\mathcal{M}_2$ being the poorest model.

Bifurcation diagrams of the original oscillator and the three models are shown in Fig. 9. Based on this figure, $\mathcal{M}_3$ seems to be the best overall model, although the several coexisting attractors make a detailed comparison difficult. The results reported in Table III and in Fig. 9 seem to confirm that the best overall model is, in fact, $\mathcal{M}_3$.

It is worth pointing out that in many other studied examples (including the ones presented in Secs. IV A 1 and IV A 2) the comparison of bifurcation diagrams was quite straightforward. In all such cases, the maximum synchronization error and the cost of synchronization consistently indicated the model with the best bifurcation diagram. However, the comparison of bifurcation diagrams in this example is particularly subjective. It would be hard to state that the diagram in Fig. 9(c) is "good," but it is easier to accept that it is closer to the original diagram in Fig. 9(d) than the first two, Figs. 9(a) and 9(b). The subjectivity in the comparison of bifurcation diagrams is, in fact, a major motivation to follow the method proposed in this paper.

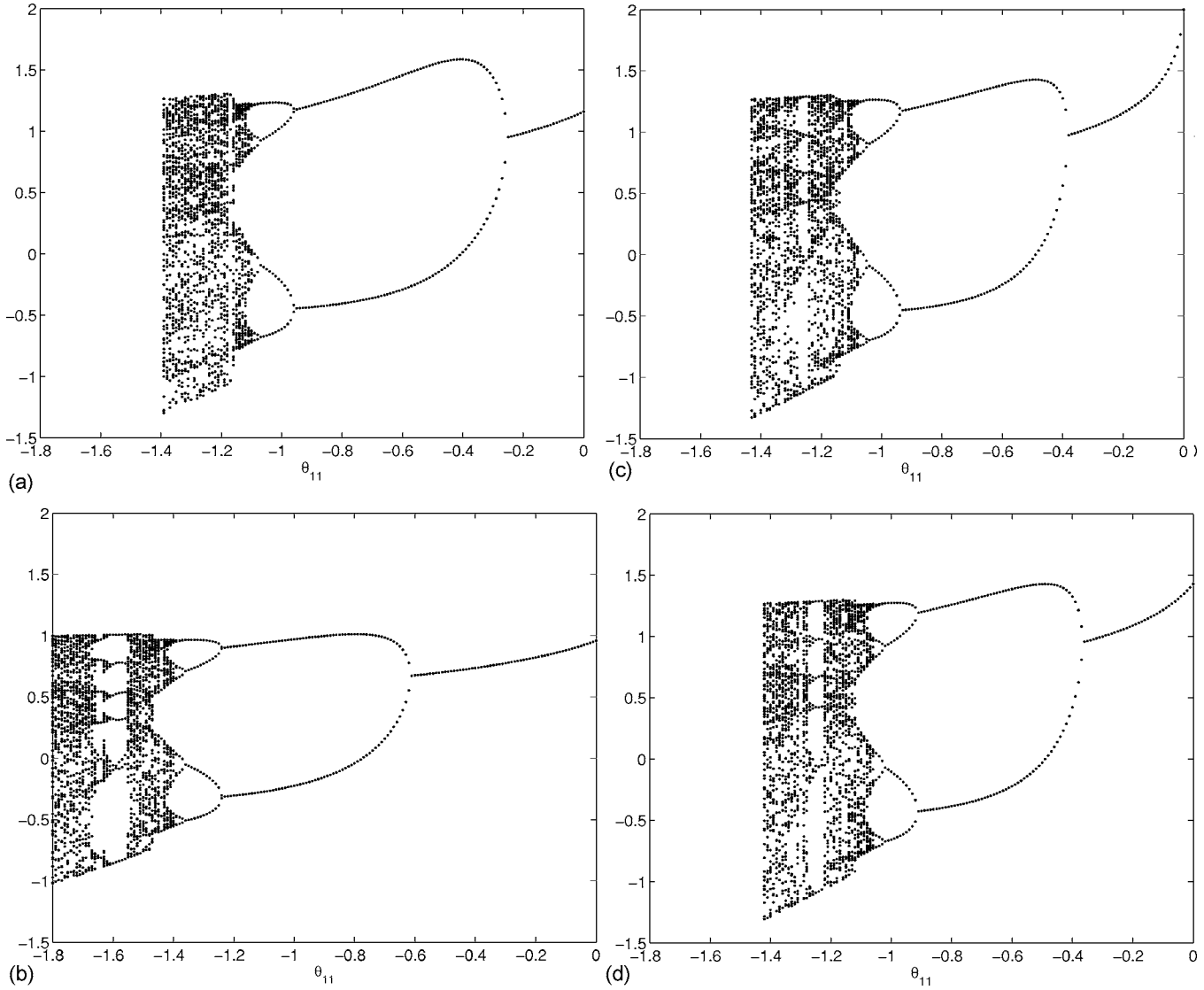

FIG. 10. Bifurcation diagrams for the example with the Hénon map: (a) $\mathcal{M}_1$, (b) $\mathcal{M}_2$, (c) $\mathcal{M}_3$, and (d) original map. All the maps use $y(k-1)^2$ as an independent variable (i.e., in the domain of the map). The associated parameter has been labeled θ_{11}. For the original map $\theta_{11}=\beta$.

C. Hénon map

This example considers a two-dimensional autonomous system, the Hénon map [67]:

$$y(k) = 1 + 0.3y(k-2) + \beta y(k-1)^2, \tag{11}$$

which settles to a chaotic attractor for $\beta=-1.4$. The bifurcation diagrams of map (11) and of other three (similar) maps are shown in Fig. 10. A glance at Fig. 10 suggests that, among the three models considered, the bifurcation of $\mathcal{M}_3$ is closest to that of the original map. This conclusion can be arrived at, at a much lower computational cost, by using the procedure proposed in this paper which yields the results shown in Fig. 11. From that figure it is readily seen that $\mathcal{M}_3$ has the smallest maximum normalized synchronization error ($\min[\epsilon_m^3] \approx 0.08$).

V. DISCUSSION AND CONCLUSIONS

The issue of model evaluation has been addressed in this paper. An overall look at the literature in the field of nonlinear dynamics has been presented. Aspects of model evaluation, such as forecasting performance (i.e., free-run predictions errors) and geometrical performance (i.e., correlation dimension of model attractors), have received due attention in the literature. On the other hand, important though it is, it is the authors' impression that the issue of comparing model *dynamical* performance is relatively neglected in the literature.

Many of the "absolute" measures that are currently used to compare models are, in a sense, geometrical rather than dynamical. A truly dynamical approach to model characterization can be achieved by means of topological analysis. However, such a procedure is known to be very intensive, time consuming, is limited to systems of dimension up to 3

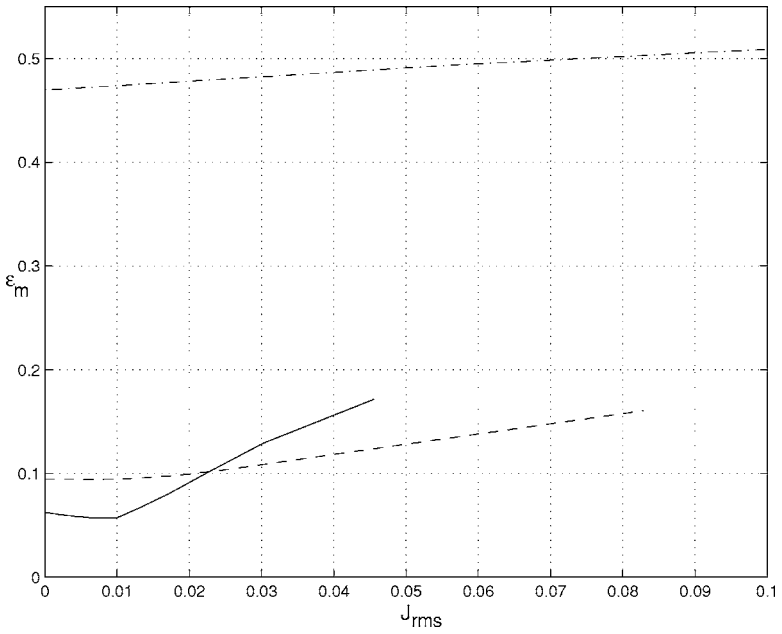

FIG. 11. Maximum normalized synchronization error $\epsilon_m(c)$ against the cost of synchronization, $J_{rms}(c)$, for Hénon models: (dashed line) $\mathcal{M}_1$, (dot-dashed line) $\mathcal{M}_2$, and (solid line) $\mathcal{M}_3$. Each point on the lines corresponds to a particular value of c which was varied in the range $0 \leq c \leq 0.9$.

and requires rather large ($\sim$100 cycles) amounts of oversampled and stationary data. The payoff for such an effort is that the template and bifurcation patterns of a system are connected and, even more, a template can be validated in absolute (rather than relative) terms [66]. In practice this means that a template can be declared valid, rather than "better than" some other template.

After comparison of some procedures for model evaluation commonly used a decade ago (and the overall scenario is very much the same today), it was concluded that bifurcation diagrams had high discriminating power due to the fact that they describe the sequence of dynamic regimes over a wide range of parameter values [3]. Such a procedure, however, has two main practical drawbacks. In the first place, and probably the most serious one, it is not always viable to obtain a bifurcation diagram directly from the original system in order to serve as a standard. In the second place, to produce bifurcation diagrams could become time consuming and subjective. Therefore, to use bifurcation diagrams as a criterion for model evaluation, in an automatic setting, does not seem feasible at the moment.

This paper has also pointed out three specific potential procedures for model evaluation: a synchronization-based scheme [55], a surrogate-based view of the problem [52], and, more recently, an approach based on testing for consistent predictions [54]. All these methods are rather subjective. Also such approaches seem to be better suited for comparing models rather than for declaring a model "valid," which would not be the best way of looking at the problem anyway [74].

In the context of this paper, special attention is given to the synchronization procedure originally suggested in [55]. The underlying thought in that work was that valid models can be made to synchronize with the data. One of the practical difficulties with this approach, which was developed for continuous-time models, is that even poor models can be forced to synchronize. Hence, under a stronger synchronizing drive, an "invalid" model can be declared "valid." This might account for the fact that the mentioned procedure has not been used in the realm of model validation.

This paper proposed and discussed a method for model evaluation that will find its roots in [55]. Some important modifications were carried out in order to overcome some of the major difficulties of the former work. First, a synchronization scheme suitable for discrete-time models was developed. Second, rather than approaching the problem of model validation from a "synchronize versus nonsynchronize" viewpoint, the model evaluation carried out in this paper assesses the *quality* and *cost* of synchronization. In this paper such features were considered, in a sense, independently. It would be interesting to have a single composite measure that combined both. This is left for the future.

The procedure has been tested for three well-known nonlinear oscillators for which detailed bifurcation diagrams can be obtained. In this framework there is *no need* for bifurcation diagrams. However, because of the high discriminating power of such diagrams, they were used as a means to assess the main features of the synchronization-based scheme. In all cases studied great consistency was found in the results using bifurcation diagrams and our scheme. It is believed that the method proposed in this paper, in what concerns model comparison, is almost as effective as the use of bifurcation diagrams but with the advantage that computation time could be two or even three orders of magnitude shorter than in the case of bifurcation diagrams.

Finally, the authors are not aware of any theoretical results that could be used to prove the generality of the results reported in this paper. An interesting question would be to investigate theoretically the connection between bifurcations and synchronization. In this respect two related results are provided. First, using arguments based on shadowing theory, it has been recently concluded that the one-step-ahead prediction conveys important information on model dynamics [75] which seems to be confirmed by (4) and the subsequent

discussion. Second, for continuous-time models, it has been shown that the control action needed to achieve identical synchronization equals the vector field mismatch between the two considered systems [62]. Such a result has been recently extended to discrete-time systems, and it has been shown that the synchronization effort is a measure of the dynamical structural mismatch between the two considered systems [76]. In any case, such considerations should only be regarded as starting points for a more precise and theoretical analysis of the procedure presented in this paper.

ACKNOWLEDGMENTS

The authors are grateful to Christophe Letellier for a critical reading of the manuscript. Financial support from CNPq is gratefully acknowledged.

[1] J. P. Crutchfield and B. S. McNamara, Complex Syst. **1**, 417 (1987).
[2] P. E. Rapp, T. I. Schmah, and A. I. Mees, Physica D **132**, 133 (1999).
[3] L. A. Aguirre and S. A. Billings, Int. J. Bifurcation Chaos Appl. Sci. Eng. **4**, 109 (1994).
[4] Y. V. Kolokolov and A. V. Monovskaya, Int. J. Bifurcation Chaos Appl. Sci. Eng. **16**, 85 (2006).
[5] T. P. Lim and Puthusserypady, Chaos **16**, 013106 (2006).
[6] L. A. Aguirre, R. A. M. Lopes, G. Amaral, and C. Letellier, Phys. Rev. E **69**, 026701 (2004).
[7] L. A. Aguirre and E. M. Mendes, Int. J. Bifurcation Chaos Appl. Sci. Eng. **6**, 279 (1996).
[8] E. Bagarinao, K. Pakdaman, T. Nomura, and S. Sato, Phys. Rev. E **60**, 1073 (1999).
[9] E. Bagarinao, K. Pakdaman, T. Nomura, and S. Sato, Physica D **130**, 211 (1999).
[10] S. A. Billings and D. Coca, Int. J. Bifurcation Chaos Appl. Sci. Eng. **9**, 1263 (1999).
[11] J. H. B. Deane, Electron. Lett. **29**, 957 (1993).
[12] D. C. Hamil (unpublished).
[13] H. M. Henrique, E. L. Lima, and J. C. Pinto, Lat. Am. Appl. Res. **28**, 187 (1998).
[14] L. Le Sceller, C. Letellier, and G. Gouesbet, Phys. Lett. A **211**, 211 (1996).
[15] S. Ogawa, T. Ikeguuchi, T. Matozaki, and K. Aihara, IEICE Trans. Fundamentals **E79-A**, 1608 (1996).
[16] C. Tao, Y. Zhang, G. Du, and J. J. Jiang, Phys. Lett. A **332**, 197 (2004).
[17] R. Bakker, J. C. Schouten, C. L. Giles, F. Takens, and C. M. van den Bleek, Neural Comput. **12**, 2355 (2000).
[18] M. Small and C. K. Tse, Phys. Rev. E **66**, 066701 (2002).
[19] E. Bagarinao and S. Sato, Ann. Biomed. Eng. **30**, 260 (2002).
[20] B. P. Bezruchko and D. A. Smirnov, Phys. Rev. E **63**, 016207 (2001).
[21] A. Garulli, C. Mocenni, A. Vicino, and A. Tesi, Int. J. Bifurcation Chaos Appl. Sci. Eng. **13**, 357 (2003).
[22] G. Gouesbet and C. Letellier, Phys. Rev. E **49**, 4955 (1994).
[23] H. L. Hiew and C. P. Tsang, Inf. Sci. (N.Y.) **81**, 193 (1994).
[24] L. Jaeger and H. Kantz, Chaos **6**, 440 (1996).
[25] K. Judd and A. I. Mees, Physica D **120**, 273 (1998).
[26] C. Letellier, L. Le Sceller, G. Gouesbet, F. Lusseyran, A. Kemoun, and B. Izrar, AIChE J. **43**, 2194 (1997).
[27] U. Parlitz *et al.*, Chaos **14**, 420 (2004).
[28] P. Perona, A. Porporato, and L. Ridolfi, Nonlinear Dyn. **23**, 13 (2000).
[29] B. Pilgram, K. Judd, and A. I. Mees, Physica D **170**, 103 (2002).
[30] K. Rodríguez-Vázquez and P. J. Fleming, Knowledge Inf. Syst. **8**, 235 (2005).
[31] J. Timmer, Int. J. Bifurcation Chaos Appl. Sci. Eng. **8**, 1505 (1998).
[32] J. Timmer, H. Rust, W. Horbelt, and H. U. Voss, Phys. Lett. A **274**, 123 (2000).
[33] L. M. Pecora, T. L. Carroll, and J. F. Heagy, Phys. Rev. E **52**, 3420 (1995).
[34] K. H. Chon, J. K. Kanters, R. J. Cohen, and N. H. Holstein-Rathlou, Physica D **99**, 471 (1997).
[35] D. Coca and S. A. Billings, Phys. Lett. A **287**, 65 (2001).
[36] S. Ishii and M. A. Sato, Neural Networks **14**, 1239 (2001).
[37] E. M. A. M. Mendes and S. A. Billings, Int. J. Bifurcation Chaos Appl. Sci. Eng. **7**, 2593 (1997).
[38] E. M. A. M. Mendes and S. A. Billings, IEEE Trans. Man Cybernet.: Part A **36**, 597 (2001).
[39] L. A. Aguirre and S. A. Billings, Int. J. Bifurcation Chaos Appl. Sci. Eng. **5**, 449 (1995).
[40] D. Allingham, M. West, and A. I. Mees, Int. J. Bifurcation Chaos Appl. Sci. Eng. **8**, 2191 (1998).
[41] B. P. Bezruchko, A. S. Karavaev, V. I. Ponomarenko, and M. D. Prokhorov, Phys. Rev. E **64**, 056216 (2001).
[42] G. Boudjema and B. Cazelles, Chaos, Solitons Fractals **12**, 2051 (2001).
[43] R. Brown, V. In, and E. R. Tracy, Physica D **102**, 208 (1997).
[44] C. S. M. Lainscsek, C. Letellier, and F. Schürrer, Phys. Rev. E **64**, 016206 (2001).
[45] J. Maquet, C. Letellier, and L. A. Aguirre, J. Theor. Biol. **228**, 421 (2004).
[46] O. Ménard, C. Letellier, J. Maquet, L. Le Sceller, and G. Gouesbet, Int. J. Bifurcation Chaos Appl. Sci. Eng. **10**, 1759 (2000).
[47] C. Letellier and G. Gouesbet, J. Phys. II **6**, 1615 (1996).
[48] C. Letellier, L. Le Sceller, P. Dutertre, G. Gouesbet, Z. Fei, and J. L. Hudson, J. Phys. Chem. **A99**, 7016 (1995).
[49] N. B. Tufillaro, P. Wyckoff, R. Brown, T. Schreiber, and T. Molteno, Phys. Rev. E **51**, 164 (1995).
[50] J. Theiler, S. Eubank, A. Longtin, B. Galdrijian, and J. D. Farmer, Physica D **58**, 77 (1992).
[51] J. Timmer, Phys. Rev. E **58**, 5153 (1998).
[52] M. Small and K. Judd, Physica D **117**, 283 (1998).
[53] C. Letellier, T. D. Tsankov, G. Byrne, and R. Gilmore, Phys. Rev. E **72**, 026212 (2005).
[54] P. E. McSharry and L. A. Smith, Physica D **192**, 1 (2004).
[55] R. Brown, N. F. Rul'kov, and E. R. Tracy, Phys. Rev. E **49**, 3784 (1994).

[56] R. Brown, N. F. Rulkov, and E. R. Tracy, Phys. Lett. A **194**, 71 (1994).
[57] C. Letellier, O. Ménard, and L. A. Aguirre, in *Modeling and Forecasting Financial Data: Techniques of Nonlinear Dynamics*, edited by A. S. Soofi and L. Cao (Kluwer, Dordrecht, 2002), pp. 283–302.
[58] C. Sarasola, F. J. Torrrealdea, A. dAnjou, and M. Graña, Math. Comput. Simul. **58**, 309 (2002).
[59] U. S. Freitas, E. E. N. Macau, and C. Grebogi, Phys. Rev. E **71**, 047203 (2005).
[60] A. Maybhate and R. E. Amritkar, Phys. Rev. E **59**, 284 (1999).
[61] U. Parlitz, Phys. Rev. Lett. **76**, 1232 (1996).
[62] L. A. B. Tôrres and L. A. Aguirre, Physica D **196**, 387 (2004).
[63] L. H. A. Monteiro, N. C. F. Canto, J. G. Chaui-Berlinck, F. M. Orsatti, and J. R. C. Piqueira, IEEE Trans. Neural Netw. **14**, 1572 (2003).
[64] L. H. A. Monteiro, M. A. Bussab, and J. G. Chaui-Berlinck, J. Theor. Biol. **219**, 83 (2002).
[65] R. Femat, R. Jauregui-Ortiz, and G. Solis-Perales, IEEE Trans. Circuits Syst., I: Fundam. Theory Appl. **48**, 1161 (2001).
[66] R. Gilmore and M. Lefranc, *The Topology of Chaos* (Wiley Interscience, New York, 2002).
[67] M. Hénon, Commun. Math. Phys. **50**, 69 (1976).
[68] Y. Ueda, Int. J. Non-Linear Mech. **20**, 481 (1985).
[69] P. J. Holmes, Philos. Trans. R. Soc. London, Ser. A **292**, 419 (1979).
[70] A. Wolf, J. B. Swift, H. L. Swinney, and J. A. Vastano, Physica D **16**, 285 (1985).
[71] D. Yu, M. Small, R. G. Harrison, and C. Diks, Phys. Rev. E **61**, 3750 (2000).
[72] K. Judd, Physica D **56**, 216 (1992).
[73] Y. Ueda and N. Akamatsu, IEEE Trans. Circuits Syst. **28**, 217 (1981).
[74] K. Judd, in *Chaos and Its Reconstruction*, edited by G. Gouesbet, S. Meunier-Guttin-Cluzel, and O. Ménard (Nova Science, New York, 2003), pp. 179–214.
[75] D. Orrell, Int. J. Bifurcation Chaos Appl. Sci. Eng. **15**, 3265 (2005).
[76] L. A. B. Tôrres (unpublished).
[77] M. Small, D. Yu, and R. G. Harrison, Int. J. Bifurcation Chaos Appl. Sci. Eng. **13**, 743 (2003).
[78] G. Gouesbet, S. Meunier-Guttin-Cluzel, and O. Ménard, in *Chaos and Its Reconstruction*, edited by G. Gouesbet, S. Meunier-Guttin-Cluzel, and O. Ménard (Nova Science, New York, 2003), pp. 1–160.
[79] L. A. Aguirre and A. V. P. Souza, Comput. Biol. Med. **34**, 241 (2004).
[80] R. Femat and G. Solis-Perales, Phys. Rev. E **65**, 036226 (2002).